Articles

Synthesis, Spectroscopy, and Electrochemistry of Ternary Copper(II) Complexes with 2,2-Diphenyl-4,4,6,6-tetrakis(3,5-dimethylpyrazolyl)cyclotriphosphazene and Nitrogenous Bases. X-ray Structures of $N_3P_3Ph_2(3,5\text{-}Me_2Pz)_4{\cdot}Cu(ClO_4)_2{\cdot}2H_2O$ and $N_3P_3Ph_2(3,5\text{-}Me_2Pz)_4{\cdot}Cu(ClO_4)_2{\cdot}2ImH$

K. R. Justin Thomas, P. Tharmaraj, and V. Chandrasekhar*

Department of Chemistry, Indian Institute of Technology, Kanpur-208 016, India

C. D. Bryan and A. W. Cordes*

Department of Chemistry and Biochemistry, University of Arkansas, Fayetteville, Arkansas 72701

Received October 6, 1993®

The reaction of 2,2-diphenyl-4,4,6,6-tetrakis(3,5-dimethylpyrazolyl)cyclotriphosphazene, $N_3P_3Ph_2(3,5\text{-}Me_2Pz)_4$ (TPCTP), with copper(II) perchlorate hexahydrate affords a mononuclear coordination complex, TPCTP·Cu-$(ClO_4)_2{\cdot}2H_2O$ (**1**). This, on treatment with nitrogenous bases such as pyridine, imidazole, 2,2′-bipyridine, and 1,10-phenanthroline in appropriate proportions, yields the ternary complexes TPCTP·$Cu(ClO_4)_2{\cdot}n$L (**2**, L = Py (n = 2); **3**, L = ImH (n = 2); **4**, L = Bipy (n = 1); **5**, L = Phen (n = 1)). Optical absorption and EPR spectra of these complexes indicate a distorted tetragonal geometry around copper in all the compounds. The structures of TPCTP·$Cu(ClO_4)_2{\cdot}2H_2O$ (**1**) and TPCTP·$Cu(ClO_4)_2{\cdot}2$ImH (**3**) were determined by X-ray crystallography. Crystals of **1** were monoclinic, with the space group $P2_1/a$ and with a = 18.401(4) Å, b = 19.927(4) Å, c = 11.875(20) Å, β = 90.696(15)°, V = 4354(15) Å^3, and Z = 4. The copper atom is coordinated by two nongeminal pyrazolyl pyridinic nitrogens, two water molecules, cyclophosphazene skeletal nitrogen, and a perchlorate anion in an elongated octahedral geometry. Crystals of compound **3** were also monoclinic, with the space group $P2_1/n$ and with a = 12.121(7) Å, b = 21.110(2) Å, c = 19.464(5) Å, β = 101.39(3)°, V = 4882(3) Å^3, and Z = 4. Copper assumes a distorted square pyramidal geometry with the basal plane comprised of two pyrazolyl nitrogens and two imidazolyl nitrogens and the apical position being occupied by the cyclophosphazene ring nitrogen. The cyclophosphazene ring nitrogen–copper binding appears to be a σ-bonding interaction, as evidenced by the lengthening of the P–N bonds that flank the coordination site. Cyclic voltammetric studies have also been carried out on complexes **1**–**5**. The six-coordinate complex **1** exhibits redox potentials 0.3 V higher than the five-coordinate square pyramidal complexes.

Introduction

Inorganic heterocyclic compounds containing alternate phosphorus and nitrogen atoms, cyclophosphazenes, have been attracting widespread attention.[1,2] The major impetus for this activity is due to an intrinsic curiosity in the rich chemistry of substitution in the P–X bonds of halogenocyclophosphazenes, $[NPX_2]_n$ (X = Cl, F; n = 3, 4), by a variety of nucleophiles and the stereo- and regiochemical effects seen therein.[1,2] Another great motivation for the study of these ring systems stems from the ring-opening polymerization of $N_3P_3Cl_6$ to the linear macromolecule $[N{=}PCl_2]_n$.[1a] Allcock and co-workers have shown that the information derived from the most versatile small-molecule model systems can be applied to the poly(dichlorophosphazene).[1a] Using this approach, over 300 structurally and functionaly diverse polyphosphazenes have been synthesized.[3]

More recently there has also been considerable interest in the use of cyclophosphazenes as ligands for transition metals.[4] Although cyclophosphazenes can interact in several ways with transition metals, the most versatile method of assembling cyclophosphazene ligand systems appears to be attaching suitable side groups containing donor atoms to the phosphorus atom of the cyclophosphazene ring. Thus, cyclophosphazenes containing exocyclic phosphino, acetylinic, carboranyl, Schiff base, etc. groups have been synthesized and have been found to form transition metal complexes.[4,5] Some of these coordination compounds have been found to be active catalysts for certain organic transformations.[5]

We recently showed that the substitution of a donor group such as 3,5-dimethylpyrazolyl on phosphorus leads to novel ligands which can interact with metals *via* cyclophosphazene

---

® Abstract published in *Advance ACS Abstracts,* July 15, 1994.

(1) (a) Allcock, H. R. *Acc. Chem. Res.* **1979**, *12*, 351. (b) Allen, C. W. *Chem. Rev.* **1991**, *91*, 133. (c) Chandrasekhar, V.; Thomas, K. R. J. *Struct. Bonding* (*Berlin*) **1993**, *81*, 41.

(2) Allen, C. W. In *The Chemistry of Inorganic Homo- and Heterocycles*; Haiduc, I., Sowerby, D. B., Eds.; Academic Press: London, 1989; Vol. 2, p 501.

(3) (a) Potin, Ph.; De Jaegar, R. *Eur. Polym. J.* **1991**, *27*, 341. (b) Allcock, H. R. *Chem. Eng. News* **1985**, *63*, 22.

(4) Chandrasekhar, V.; Thomas, K. R. J. *Appl. Organomet. Chem.* **1993**, *7*, 1.

(5) (a) Allcock, H. R.; Desorcie, L. L.; Riding, G. H. *Polyhedron* **1987**, *6*, 119. (b) Allcock, H. R.; Manners, I.; Mang, M. N.; Parvez, M. *Inorg. Chem.* **1990**, *29*, 522. (c) Allcock, H. R.; Nissan, R. A.; Harris, P. J.; Whittle, R. R. *Organometallics* **1984**, *3*, 432.

0020-1669/94/1333-5382$04.50/0

ring nitrogen as well as through exocyclic donor atoms.[6] We have reported the ligating behavior of the hexasubstituted pyrazolylcyclotriphosphazene $N_3P_3(3,5\text{-}Me_2Pz)_6$ (HPCTP) toward copper salts.[6,7] It forms both mono- and dinuclear complexes, depending on the reaction conditions. We describe here the full details of an investigation of the coordination response of a tetrasubstituted pyrazolylcyclotriphosphazene, $N_3P_3Ph_2(3,5\text{-}Me_2Pz)_4$ (TPCTP), with copper(II) perchlorate hexahydrate which includes (a) the preparation and spectroscopic (IR, UV−vis, EPR) and electrochemical (cyclic and differential pulse voltammetries) characterization of the series of complexes TPCTP·$Cu(ClO_4)_2$·*n*L (L = H_2O (**1**), Py (**2**), ImH (**3**) (*n* = 2); L = Bipy (**4**), Phen (**5**) (*n* = 1)) and (b) crystal structure determinations of complexes **1** and **3**. It is of interest to ascertain the effect of the number of coordinating groups present in the cyclophosphazene unit on the ligating capabilities. TPCTP has only four exocyclic 3,5-dimethylpyrazolyl groups when compared with HPCTP, which has six.

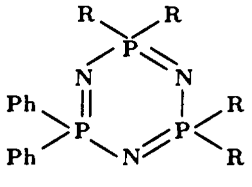

TPCTP

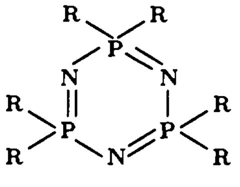

HPCTP

1 TPCTP·$Cu(ClO_4)_2$·$2H_2O$

2 TPCTP·$Cu(ClO_4)_2$·2Py

3 TPCTP·$Cu(ClO_4)_2$·2ImH

4 TPCTP·$Cu(ClO_4)_2$·Bipy

5 TPCTP·$Cu(ClO_4)_2$·Phen

6 HPCTP·$CuCl_2$

R=3,5-dimethyl-1-pyrazolyl

Experimental Section

Abbreviations. TPCTP = 2,2-diphenyl-4,4,6,6-tetrakis(3,5-dimethylpyrazolyl)cyclotriphosphazene, Bipy = 2,2′-bipyridine, Phen = 1,10-phenanthroline, Py = pyridine, ImH = imidazole, PzH = pyrazole.

Materials. The ligand TPCTP was synthesized according to the literature method.[8] 2,2′-Bipyridine, 1,10-phenanthroline, and copper(II) perchlorate hexahydrate were obtained from Aldrich Chemical Co. and used as received. NEt_4ClO_4 was a Merck product. NBu_4ClO_4 was synthesized by treating tetrabutylammonium bromide with 70% perchloric acid in water and recrystallized three times from an ethyl acetate−hexane mixture. Dichloromethane, benzene, hexane, and acetonitrile were distilled from P_2O_5 and stored over molecular sieves.

Instrumentation. Electronic absorption spectra in the 200−1100-nm range were recorded with a Shimadzu UV-160 spectrophotometer, and infrared spectra (KBr pellets), with a Perkin-Elmer Model 1320 IR spectrophotometer. The solution conductivity was measured with a Century digital conductivity meter for solute concentrations of 10^{-3} M in acetonitrile. X-band EPR spectra were obtained with a Varian spectrometer, equipped with a variable-temperature facility. The magnetic field strength was calibrated with the standard dpph (g = 2.0036). The solution magnetic moments of the samples were obtained by the Evans NMR method.[9] Electrochemical experiments were performed with a Princeton Applied Research Model 273A potentiostat/galvanostat equipped with an X-Y recorder (Digital Electronics Ltd.). Cyclic voltammograms were obtained in dichloromethane or acetonitrile solutions containing 0.1 M NBu_4ClO_4 or NEt_3ClO_4 as supporting electrolyte. The 0.001 M sample solutions were thoroughly purged with dry N_2 before each experiment. The electrochemical cell employed was of a standard three-electrode configuration: a glassy-carbon working electrode, a platinum-wire auxiliary electrode, and an aqueous Ag/AgCl reference electrode. Toward the end of each experiment, ferrocene was added as internal reference and the experiment repeated. Under this condition the Fc^+/Fc couple was located at 0.52 V in dichloromethane solution and at 0.45 V in acetonitrile solution. The half-wave potentials were reported as the average of the anodic and cathodic peak potentials of quasireversible cyclic voltammograms for a 100 mV/s scan rate. For irreverisible processes, the electrode potentials were taken from differential pulse voltammograms (scan rate 10 mV/s). Diagnostic criteria for reversibility of electron transfer processes were employed in the usual manner. Metal analyses were performed by the EDTA titration method.[10] Elemental analyses were obtained from the Microanalytical Laboratory at the Indian Institute of Technology, Kanpur, India, and the Central Drug Research Institute, Lucknow. Melting points were obtained using a Fisher-Johns hot plate and are uncorrected.

Synthesis of TPCTP·$Cu(ClO_4)_2$·$2H_2O$ (1). The ligand TPCTP (0.669 g, 1 mmol) and $Cu(ClO_4)_2$·$6H_2O$ (0.37 g, 1 mmol) were stirred in dichloromethane (20 mL) for 1 h. A light blue solution resulted, which was concentrated to *ca.* 5 mL, and diethyl ether (20 mL) was added. A blue microcrystalline solid was obtained, washed with benzene, dried over dry $CaCl_2$, and recrystallized from a dichloromethane−benzene (1:1) mixture (0.9 g, 93% yield). Mp: 208 °C. Anal. Calcd for $C_{32}H_{42}N_{11}P_3O_{10}CuCl_2$: C, 39.67; H, 4.37; N, 15.92; Cu, 6.56. Found: C, 39.62; H, 4.40; N, 15.81; Cu, 6.45. Conductivity (mhos cm^2 mol^{-1}, CH_3CN): 240. IR (KBr, cm^{-1}): 3400 br, 1562 s, 1460 m, 1453 m, 1445 m, 1430 m, 1405 m, 1310 sh, 1225 vs, br, 1180 vs, 1100 vs, br, 1040 s, 990 w, 980 w, 965 m, 915 w, 870 m, 820 w, br, 768 w, 740 m, 720 m, 720 s, 690 m, 620 s.

Synthesis of Ternary Complexes with Nitrogen Heterocyclic Bases. A typical procedure is given below.

TPCTP·$Cu(ClO_4)_2$·Bipy (4). The complex TPCTP·$Cu(ClO_4)_2$·$2H_2O$ (**1**) (0.194 g, 0.2 mmol), prepared in situ, was treated with an equivalent amount of 2,2′-bipyridine (0.031 g, 0.2 mmol) in dichloromethane (20 mL) for 30 min with vigorous stirring. The resulting deep blue solution was filtered, the filtrate was evaporated to *ca.* 5 mL, and diethyl ether (15 mL) was added. A blue precipitate formed, which was washed with benzene and hexane, dried over dry $CaCl_2$, and finally recrystallized from a dichloromethane−hexane (1:1) mixture (0.198 g, 91% yield). Mp: 152 °C dec. Anal. Calcd for $C_{42}H_{46}N_{13}P_3O_8CuCl_2$: C, 46.37; H, 4.26; N, 16.74; Cu, 5.84. Found: C, 46.20; H, 4.23; N, 16.89; Cu, 5.68. Conductivity (mhos cm^2 mol^{-1}, CH_3CN): 265. IR (KBr, cm^{-1}): 1600 m, 1570 s, 1478 m, 1467 m, 1459 m, 1440 s, 1410 m, 1310 m, 1290 s, 1230 vs, br, 1180 s, 1150 sh, 1090 vs, br, 1050 sh, 960 m, 865 w, br, 770 m, 740 sh, 730 m, 690 w, br, 625 s.

Other complexes were obtained by adopting a similar method, except in case of monodentate ligands 2 equiv of base was consumed. Analytical details for these complexes are as follows:

TPCTP·$Cu(ClO_4)_2$·2Py (2). Yield: 80%. Mp: 140 °C. Anal. Calcd for $C_{42}H_{48}N_{13}P_3O_8CuCl_2$: C, 46.28; H, 4.44; N, 16.71; Cu, 5.83. Found: C, 46.35; H, 4.35; N, 16.93; Cu, 5.80. Conductivity (mhos cm^2 mol^{-1}, CH_3CN): 235. IR (KBr, cm^{-1}): 1595 m, 1560 s, 1440 s, 1430 s, 1400 m, 1360 m, 1310 sh, 1285 s, 1230 vs, br, 1175 s, 1080 s, br, 1040 sh, 950 m, 860 w, br, 732 m, 720 m, 690 m, 618 s.

TPCTP·$Cu(ClO_4)_2$·2ImH (3). Yield: 95%. Mp: 213 °C. Anal. Calcd for $C_{38}H_{46}N_{15}P_3O_8CuCl_2$: C, 42.73; H, 4.34; N, 19.67; Cu, 5.95. Found: C, 42.35; H, 4.38; N, 19.57; Cu, 6.03. Conductivity (mhos cm^2 mol^{-1}, CH_3CN): 250. IR (KBr, cm^{-1}): 3300 s, br, 1560 m, 1530 m, 1450 s, 1427 s, 1400 m, 1360 w, 1310 sh, 1283 s, 1225 vs, br, 1170 s, 1100 vs, br, 1050 sh, 960 sh, 950 m, 860 m, 800 w, br, 750 m, 745 m, 730 s, 720 s, 682 m, 640 m, 610 s.

TPCTP·$Cu(ClO_4)_2$·Phen (5). Yield: 86%. Mp: 168 °C. Anal. Calcd for $C_{44}H_{46}N_{13}P_3O_8CuCl_2$: C, 47.51; H, 4.17; N, 16.37; Cu, 5.71. Found: C, 47.30; H, 4.23; N, 16.25; Cu, 5.65. Conductivity (mhos

---

(6) Thomas, K. R. J.; Chandrasekhar, V.; Pal, P.; Scott, S. R.; Hallford, R.; Cordes, A. W. *Inorg. Chem.* **1993**, *32*, 606.

(7) Thomas, K. R. J.; Chandrasekhar, V.; Scott, S. R.; Hallford, R.; Cordes, A. W. *J. Chem. Soc., Dalton Trans.* **1993**, 2589.

(8) Gallicano, K. D.; Paddock, N. L. *Can. J. Chem.* **1982**, *60*, 521.

(9) Evans, D. F. *J. Chem. Soc.* **1959**, 2003.

(10) Jeffery, G. H.; Bassett, J.; Mendham, J.; Denney, R. C. *Vogel's Textbook of Quantitative Chemical Analysis*, 5th ed.; ELBS/Longman: London, 1989.

Table 1. Crystallographic Details for Complexes **1** and **3**

	1	**3**
formula	$CuCl_2P_3O_{10}N_{11}C_{32}H_{42}$	$CuCl_2P_3O_8N_{15}C_{38}H_{46}$
fw	968.11	1068.23
crystal color	blue	blue
crystal dimens, mm^3	0.60 × 0.66 × 0.70	0.14 × 0.13 × 0.56
space group	$P2_1/a$	$P2_1/n$
a, Å	18.401(4)	12.121(7)
b, Å	19.927(4)	21.110(2)
c, Å	11.875(20)	19.464(5)
β, deg	90.696(15)	101.39(3)
V, $Å^3$	4354(15)	4882(3)
μ, mm^{-1}	0.79	0.72
Z	4	4
$F(000)$	2000.06	2208.1
d_{calcd}, g cm^{-3}	1.48	1.45
T, K	293	293
λ, Å	0.710 73	0.710 73
no. of unique reflns	5665	4544
no. of obsd reflns	3918 ($I > 3\sigma(I)$)	2950 ($I > 2.5\sigma(I)$)
GOF	1.26	1.12
P	0.0025	0.05
Δ/σ (max)	0.08	0.001
R^a	0.048	0.049
$R_w{}^b$	0.072	0.067

[a] $R = [\Sigma||F_o| - |F_c||]/[\Sigma|F_o|]$. [b] $R_w = \{[\Sigma w||F_o| - |F_c||^2]/[\Sigma w|F_o|^2]\}^{1/2}$.

cm^2 mol^{-1}, CH_3CN): 272. IR (KBr, cm^{-1}): 1565 s, 1510 m, 1450 m, 1425 m, 1405 m, 1305 sh, 1290 s, 1230 vs, br, 1180 s, 1150 s, 1080 vs, br, 1040 sh, 1020 sh, 951 s, 865 m, 840 m, 800 w, br, 735 s, 725 s, 712 s, 690 m, 620 s.

Caution! Although the perchlorate complexes reported in this study were not found to be shock sensitive, the materials should be handled with extreme care in small quantities.

X-ray Crystallography. The structures of **1** and **3** were solved by direct methods (SHELX 86).[11] Refinements of the structures were performed by the full-matrix least-squares method, first with isotropic and subsequently with anisotropic temperature factors for the non-hydrogen atoms. Most hydrogen atoms were located on a difference Fourier map. The hydrogen atoms were ultimately included with their positions calculated using sp^3 or sp^2 hybridization at the appropriate C atom with a fixed C−H distance of 0.95 Å or N atom with an N−H distance of 0.90 Å; the hydrogen atoms found served to determine the conformation of the methyl groups. These were included in the subsequent cycles of refinement with isotropic temperature factors. Refinements converged with $R = 0.048$ and $R_w = 0.072$ (for complex **1**) and $R = 0.049$ and $R_w = 0.067$ (for **3**). In the refinement cycles, weights were derived from the counting statistics. Scattering factors were taken from ref 12. The final difference map calculated at the conclusion of the refinement had no chemically significant features. The computer program used was NRC 386 (PC version of NRCVAX).[13]

X-ray Analysis of TPCTP·Cu(ClO_4)$_2$·2H_2O (1). A blue crystal (0.60 × 0.66 × 0.70 mm^3) of **1** was mounted on a fiber with epoxy on a CAD-4 Enraf-Nonius diffractometer. The cell parameters were obtained by a least-squares fit of 25 reflections (2θ range: 20−22°). Crystal parameters are given in Table 1. Data were collected by the $\theta-2\theta$ scan technique with graphite-monochromated Mo Kα radiation, a scan speed of 4−16°/min, and a scan width of $(1.0 + 0.35 \tan\theta)°$ with $h = -19$ to $+19$, $k = 0$ to 21, $l = 6$ to 12. Three reflections were monitored every 2 h of exposure time and showed insignificant variations. The intensities of 5984 reflections were measured, of which 3918 had $I > 3\sigma(I)$. Data were corrected for Lorentz, polarization, and absorption effects, the correction range for absorption being 0.85−1.00. The perchlorate anions were treated with idealized bond lengths (1.414 Å) and bond angles (109.5°) and without disorder in oxygen atom positions.

X-ray Analysis of TPCTP·Cu(ClO_4)$_2$·2ImH (3). A suitable blue crystal (0.14 × 0.13 × 0.56 mm^3) of **3** obtained by slow diffusion of benzene into a dichloromethane solution of **3** was glued with epoxy onto a glass fiber and transferred to an Enraf-Nonius CAD-4 diffractometer. Unit cell dimensions were determined from 25 reflections in the 2θ range 16−18.5°. Intensity data were collected by the $\theta-2\theta$ scan method for the variable scan speed 4−16°/min, a scan width of $(1.0 + 0.35 \tan\theta)°$, and graphite-monochromated Mo Kα radiation in the 2θ range 4−40° with $h = -11$ to $+11$, $k = 0$ to 20, $l = 0$ to 18. The intensities of 4544 unique reflections were measured, of which 2950 had $I > 2.5\sigma(I)$. Data were corrected for Lorentz, Polarization, and absorption (empirical ψ scans) effects, the correction range for absorption being 0.88−1.00. Perchlorate anions were modeled as two rigid groups in the ratio 0.85:0.15. Crystal data are given in Table 1.

Results and Discussion

Synthesis. The ligand 2,2-diphenyl-4,4,6,6-tetrakis-(3,5-dimethylpyrazolyl)cyclotriphosphazene is readily obtained by treating $N_3P_3Ph_2Cl_4$ with 3,5-dimethylpyrazole in the presence of a slight excess of triethylamine. It functions as a novel tridentate N_3 donor ligand toward transition metals. TPCTP reacts with copper(II) perchlorate hexahydrate to yield the hexacoordinated copper complex TPCTP·Cu(ClO_4)$_2$·2H_2O (**1**) (Scheme 1). This complex serves as an intermediate for the preparation of a series of ternary complexes with additional bidentate or monodentate nitrogeneous bases (Scheme 1). Thus, **1** reacts with 2 equiv of imidazole or pyridine or 1 equiv of 2,2′-bipyridine or 1,10-phenanthroline to form the corresponding mixed-ligand complexes, TPCTP·Cu(ClO_4)$_2$·nL (L = Py (**2**) or ImH (**3**) and $n = 2$; L = Bipy (**4**) or Phen (**5**) and $n = 1$), *via* the expulsion of the coordinated aquo ligands (Scheme 1). This is reflected in the disappearance of the broad absorption centered at 3400 cm^{-1} in the IR spectra of complexes **2**−**5** in contrast to the spectrum of the former (**1**).

It is believed that the splitting of the P=N stretching frequency is suggestive of cyclophosphazene ring nitrogen coordination to the metal.[1] For the ligand (TPCTP) a single broad P=N stretching band is observed at 1220 cm^{-1} which is split into two components for all the complexes; these occur at *ca.* 1230 and 1180 cm^{-1}, respectively, indicative of phosphazene ring nitrogen participation in coordination. The observation of singlets at *ca.* 1040 cm^{-1} and another at *ca.* 620 cm^{-1} establishes the presence of uncoordinated perchlorate anions in the ternary complexes.[14] This is also evident from the unsplit ν_3(ClO_4) singlet at *ca.* 1080 cm^{-1}. The conductivity data for complexes **1**−**5** indicate that in acetonitrile solution they behave as 1:2 electrolytes, in the range 220−280 mhos cm^2 mol^{-1}. The magnetic moments calculated by using the Evans NMR method[9] fall within the range 1.80−2.00 μ_B (Table 2) and are normal for five- and six-coordinate copper(II) complexes.[15]

X-ray Crystal Structures of TPCTP·Cu(ClO_4)$_2$·2H_2O (1) and TPCTP·Cu(ClO_4)$_2$·2ImH (3). The ORTEP drawings[16] of **1** and **3** with the atomic numbering schemes are displayed in Figures 1 and 2, respectively. Selected bond lengths and bond angles are given in Table 3. These are the first examples of the crystal structures of copper ternary complexes with any cyclophosphazene ligand systems.

The copper in complex **1** adopts an elongated octahedral geometry with the cyclophosphazene skeletal nitrogen and a perchlorate anion occupying the axial positions. The basal plane

---

(11) Sheldrick, G. M. SHELX86: Program for the Automatic Solution of Crystal Structure. University of Göttingen, Germany, 1986.

(12) *International Tables for X-ray Crystallography*; Kynoch Press: Birmingham, England, 1974; Vol. IV.

(13) Gabe, E. J.; Le Page, Y.; Charland, J.-P.; Lee, F. L.; White, P. S. *J. Appl. Crystallogr.* **1989**, *22*, 383.

(14) Nakamato, K. *Infrared Spectra of Inorganic and Coordination Compounds*; Wiley-Interscience: New York, 1970; p 175.

(15) (a) Hathaway, B. J.; Billing, D. E. *Coord. Chem. Rev.* **1970**, *5*, 143. (b) Hathaway, B. J. *Struct. Bonding (Berlin)* **1984**, *57*, 55.

(16) Johnson, C. K. ORTEP II. Report ORNL-5138; Oak Ridge National Laboratory: Oak Ridge, TN, 1976.

Scheme 1

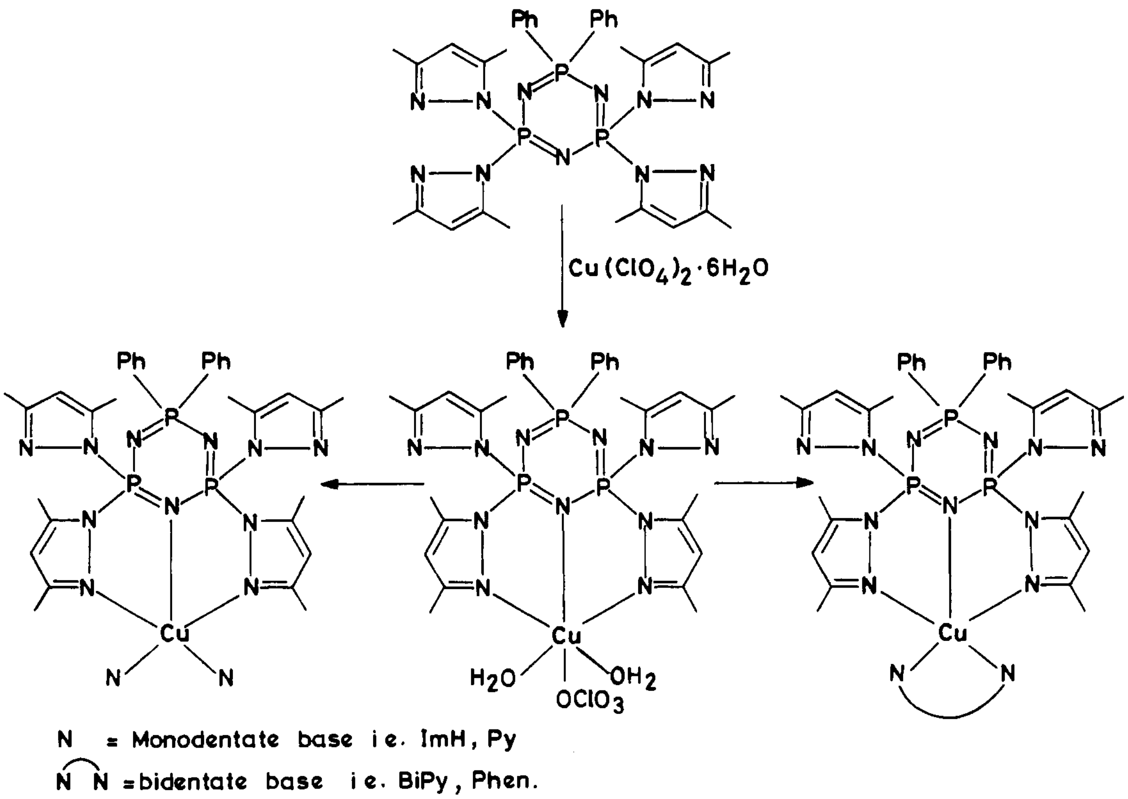

Table 2. Magnetic and Electronic Spectral Data

compd	solvent	μ_{eff}, μ_B	λ_{max}, nm (ϵ, M^{-1} cm^{-1} × 10^3) d–d	LMCT	π–π* intraligand
1	CH_2Cl_2	1.79	764 (0.13)	265 (2.6) 364 (1.56)	236 (24.0)
	CH_3CN		726 (0.12)	267 (2.45) 360 (1.32)	226.5 (24.5)
2	CH_2Cl_2	1.84	657 (0.098) 775 sh	260 (2.7) 355 (1.4)	235.5 (22.0)
	CH_3CN		678 (0.1) 830 sh	263 (2.68) 358 (1.43)	225 (21.6)
3	CH_2Cl_2	1.82	637 (0.115) 830 sh	270 (2.8) 360 (1.7)	234 (28.0)
	CH_3CN		634 (0.105) 810 sh	263 (2.95) 361 (1.68)	227 (28.8)
4	CH_2Cl_2	1.88	598 (0.078) 688 (0.074)	260 sh 320 sh 365 (7.5)	237.5 (38.0)
	CH_3CN		598 (0.076) 680 (0.78)	259 (3.02) 312 sh 370 (8.2)	228 (38.0)
5	CH_2Cl_2	1.9	592 (0.062) 685 (0.064)	278 (9.6) 300 sh 370 (4.5)	236 (34.0)
	CH_3CN		580 (0.060) 676 (0.58)	280 (10.22) 305 sh 372 (5.45)	226 (32.4)

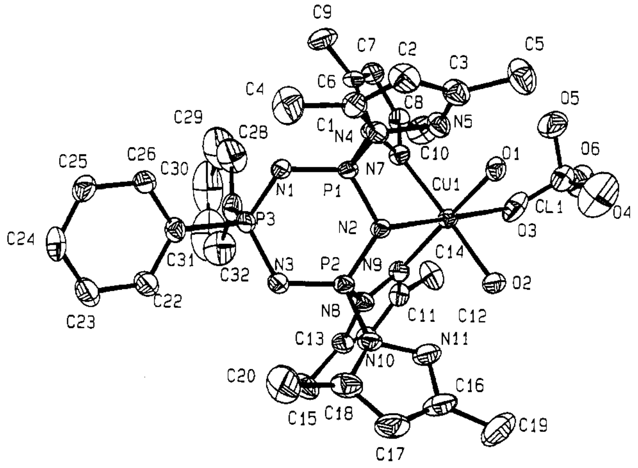

Figure 1. ORTEP diagram of compound **1**.

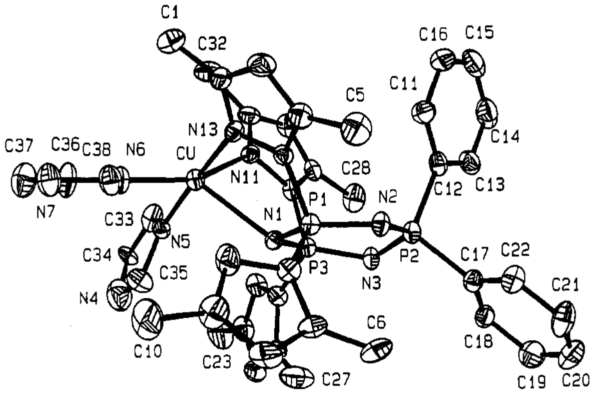

Figure 2. ORTEP diagram of compound **3**.

is constituted by two nongeminal pyrazolyl pyridinic nitrogens and two water molecules and shows slight tetrahedral distortion (Figure 1). The mean Cu–N_{pz} bond distance 2.024(5) Å is comparable to those of other related derivatives.[6,7] The Cu–O(3) distance is similar to those found for weakly coordinated axial anions or water.[17] It may be pointed out that the metal–cyclophosphazene ring nitrogen interaction is remarkably weak (2.383(4) Å) and the bond distance is even longer (~0.02 Å) than that observed in the complex HPCTP·$CuCl_2$ (**6**).[6]

---

[17] Gazo, J.; Bersuker, I. B.; Garaj, J.; Kabesoha, M.; Kohout, J.; Langfelderova, H.; Melink, M.; Serator, M.; Valach, F. *Coord. Chem. Rev.* **1976**, *19*, 253.

Table 3. Selected Bond Distances (Å) and Bond Angles (deg)

	1	3
Cu−N(2)	2.383(4)	
Cu−N(7)	2.037(5)	
Cu−N(9)	2.010(5)	
Cu−N(1)		2.325(6)
Cu−N(11)		2.076(7)
Cu−N(13)		2.014(7)
Cu−N(5)		1.968(7)
Cu−N(6)		1.981(7)
Cu−O(1)	1.964(4)	
Cu−O(2)	1.990(4)	
Cu−O(3)	2.506(5)	
P(1)−N(1)	1.568(5)	1.590(6)
P(1)−N(2)	1.593(4)	1.569(7)
P(2)−N(2)	1.589(4)	1.600(7)
P(2)−N(3)	1.558(5)	1.607(7)
P(3)−N(1)	1.617(5)	1.605(6)
P(3)−N(3)	1.615(5)	1.558(7)
O(1)−Cu−O(2)	90.44(17)	
O(1)−Cu−N(2)	93.46(15)	
O(1)−Cu−N(7)	88.20(18)	
O(1)−Cu−N(9)	173.68(17)	
O(1)−Cu−O(3)	83.89(17)	
O(2)−Cu−N(2)	96.75(16)	
O(2)−Cu−N(7)	175.38(18)	
O(2)−Cu−N(9)	86.67(18)	
O(2)−Cu−O(3)	82.67(16)	
N(2)−Cu−N(7)	78.93(16)	
N(2)−Cu−N(9)	81.31(16)	
N(2)−Cu−O(3)	177.27(16)	
N(7)−Cu−N(9)	94.24(19)	
N(7)−Cu−O(3)	101.57(17)	
N(9)−Cu−O(3)	101.30(19)	
N(1)−Cu−N(5)		96.4(3)
N(1)−Cu−N(6)		125.2(3)
N(1)−Cu−N(11)		78.8(2)
N(1)−Cu−N(13)		80.8(2)
N(5)−Cu−N(6)		88.8(3)
N(5)−Cu−N(11)		88.3(3)
N(5)−Cu−N(13)		176.1(3)
N(6)−Cu−N(11)		156.0(3)
N(6)−Cu−N(13)		90.7(3)
N(11)−Cu−N(13)		93.7(3)
N(1)−P(1)−N(2)	119.44(44)	119.1(3)
N(2)−P(2)−N(3)	119.45(24)	114.3(3)
N(1)−P(3)−N(3)	113.9(3)	117.3(3)
P(1)−N(1)−P(3)	118.9(3)	119.2(4)
P(1)−N(2)−P(2)	119.4(3)	122.1(4)
P(2)−N(3)−P(3)	119.5(3)	120.3(4)

The geometry of the copper in **3** is best described as a distorted square pyramid with the pyrazolyl groups and imidazole ligands occupying the basal positions. The apical position is occupied by the cyclophosphazene ring nitrogen. The copper−phosphazene skeletal nitrogen bond distance is considerably shorter (~0.058 Å) than those found in **1**, indicating slightly improved interaction. The mean Cu−N_{pz} and Cu−N_{im} bond distances are 2.045(7) and 1.975(7) Å, respectively, and are consistent with those observed for analogous complexes.[6,7] The Cu−N_{pz} bond distances in **1** are slightly shorter (~0.02 Å) than those in **3**, suggesting more pronounced covalent π bonding in the Cu−N_{pz} bonds of **1** attributable to the presence of less electron rich aquo ligands. An inspection of L_{ax}−Cu−L_{eq} angles reveals that the square plane around copper is severely distorted. For example the O(2)−Cu−N(2) angle in **1** is 96.75(16)° and the N(6)−Cu−N(1) angle in **3** is 125.2(3)°, suggesting that the distortion in the latter complex is toward trigonal bipyramidal geometry and accounts well the small $|A_{\parallel}|$ values observed for these complexes in the EPR spectroscopy (*vide infra*).

The cyclophosphazene skeletal bond lengths and bond angles in complexes **1** and **3** show the trends that are expected upon skeletal nitrogen coordination to the metal.[1] The P−N bonds flanking the coordination site are slightly longer than those observed for cyclophosphazenes, suggesting that the metal−skeletal nitrogen interaction is of the σ type and the lone pair electrons on nitrogens are no longer available for skeletal π bonding in the P−N(Cu)−P segment. The other P−N bond lengths are comparable to those in $N_3P_3Ph_2Cl_4$.[18] The endocyclic angles at phosphorus and nitrogen are unexceptional.[1,2] The planarity of the cyclophosphazene ring is affected by the skeletal nitrogen coordination to the metal. To relieve the strain produced by the geometrical constraint, the noncoordinated skeletal nitrogens are pushed away from the plane defined by the remaining atoms. Thus, the nitrogen atoms N(1) and N(3) in **1** are −0.258(5) and −0.252(5) Å, respectively, away from the plane defined by P(1), P(2), P(3), and N(2). However, in **3** only N(3) is projected 0.305(7) Å from the plane defined by P(1), P(2), P(3), N(1), and N(2).

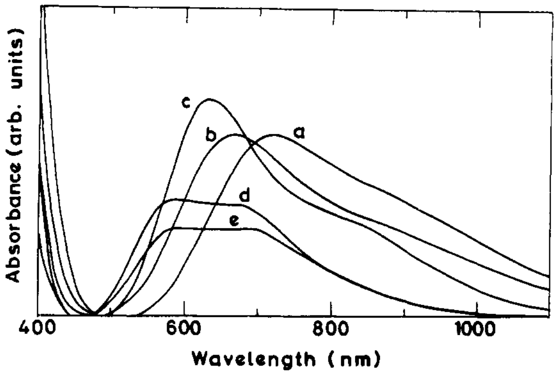

Figure 3. d−d spectra of the complexes (**1**−**5**) in acetonitrile solution (a−e).

Electronic Spectroscopy. The electronic spectral data for compounds **1**−**5** in dichloromethane and acetonitrile solutions are presented in Table 2. The high-energy transition observed at *ca.* 230 nm is assigned to the intraligand π−π^* transition. The other high-energy transitions located between 260 and 380 nm are attributed to various ligand to metal charge transfer transitions, in accordance with our previous results.[6,7] For the series of TPCTP·Cu$(ClO_4)_2$·nL complexes the intensity of the band between *ca.* 260 and 360 nm increases as the aquo ligand is replaced by the nitrogen heterocyclic ligands. The maximum increase in intensity is noticed for the 1,10-phenanthroline adduct (Table 2), indicating the additional contribution from the N(heterocycle) → Cu LMCT.

The complexes TPCTP·Cu$(ClO_4)_2$·2L exhibit a rather broad absorption band with a low-energy shoulder typical of tetragonal complexes,[15] while the 2,2′-bipyridine and 1,10-phenanthroline adducts TPCTP·Cu$(ClO_4)_2$·L show two overlapping bands of comparable intensities (Figure 3). Utilizing the energy ranges[19] covered by the d−d transitions of CuN_4−N_6 chromophores of varying stereochemistries, it is reasonable to conclude that in the present case the CuN_5 chromophore containing complexes (**2**−**5**) fall in the class of distorted square pyramidal, the distortion being toward a tetrahedral arrangement of the basal ligands. There is an apparent trend in the spectral properties of compounds **1**−**5** related to the ligand field strength of the exogenous ligands. As the aquo ligands are replaced with nitrogenous bases, the absorption maxima of the complexes shift progressively to higher energies. For instance, TPCTP·Cu$(ClO_4)_2$·$2H_2O$ (**1**) in dichloromethane solutions shows the absorption maximum centered at 764 nm while TPCTP·Cu$(ClO_4)_2$·2ImH (**3**) gives a band at 637 nm with the low-energy

---

[18] Mani, N. V.; Ahmed, F. R.; Barnes, W. H. *Acta Crystallogr.* **1965**, *19*, 693.

[19] Hathaway, B. J. *J. Chem. Soc., Dalton Trans.* **1972**, 1196.

Table 4. EPR Spin Hamiltonian Parameters[a]

compd	medium	$g_\parallel$	$g_\perp$	$\lvert A_\parallel \rvert$	g_{iso}	$\lvert A_{iso} \rvert$	$g_{av}{}^b$	G^c	$g_\parallel/\lvert A_\parallel \rvert$, cm
1	solid (rt)	2.358	2.078	131	2.171		2.175	4.711	181
	solid (lnt)	2.354	2.073	135	2.166		2.171	5.000	174
	CH_2Cl_2	2.305	2.069	149	2.166	56	2.151	4.512	154
	CH_3CN	2.365	2.072	121	2.127	56	2.174	5.213	195
2	solid (rt)	2.267	2.078	145	2.141		2.143	3.482	157
	solid (lnt)	2.277	2.072	145	2.140		2.142	3.940	158
	CH_2Cl_2	2.269	2.066	154	2.153	62	2.135	4.217	147
	CH_3CN	2.254	2.069	159	2.153	56	2.132	3.783	142
3	solid (rt)	2.260	2.053	159	2.122		2.124	5.070	143
	solid (lnt)	2.256	2.045	163	2.116		2.118	5.898	138
	CH_2Cl_2	2.265	2.062	145	2.151	65	2.132	4.376	157
	CH_3CN	2.265	2.066	145	2.152	61	2.134	4.156	157
4	solid (rt)	2.252	2.060	168	2.124		2.126	4.319	134
	solid (lnt)	2.245	2.055	168	2.119		2.121	4.579	134
	CH_2Cl_2	2.234	2.050	168	2.140	79	2.113	4.904	133
	CH_3CN	2.237	2.042	170	2.139	79	2.109	5.887	132
5	solid (rt)	2.256	2.056	163	2.123		2.125	4.705	138
	solid (lnt)	2.245	2.055	168	2.116		2.118	4.916	134
	CH_2Cl_2	2.242	2.043	168	2.141	76	2.111	5.907	134
	CH_3CN	2.238	2.049	168	2.139	75	2.114	5.035	133

[a] All the data reported here were obtained by computer simulation[7] of the experimental spectra. g_{iso} and $|A_{iso}|$ values are from room-temperature isotropic spectra for solution samples, and $g_{iso} = {}^1/_3(g_\parallel + 2g_\perp)$ for solid spectra. $|A|$ values have 10^{-4} cm^{-1} units. [b] From $[{}^1/_3(g_\parallel{}^2 + 2g_\perp{}^2)]^{1/2}$. [c] From $(g_\parallel - 2.0023)/(g_\perp - 2.0023)$.

shoulder centered at 830 nm. The data suggest, therefore, that the ligand field strengths of the exogenous ligands increase in the order H_2O < Py < ImH < Bipy ≃ Phen. Theories on the intensity of ligand absorption bands predict that the intensity of d−d transition increases as the symmetry of the ligand field decreases, since the d−d transitions become allowed as electric dipole transitions.[20] A closer inspection of Table 2 indicates that the intensities of the complexes decrease on moving from **1** to **5**. This is corroborated by the tetrahedral distortion observed by X-ray crystallography for complexes **1** and **3** (*vide supra*).

Electron Paramagnetic Resonance Spectroscopy. The X-band EPR spectra of the powdered and solution samples of **1**−**5** have been recorded both at room and liquid nitrogen temperatures. The spin Hamiltonian parameters of complexes **1**−**5** are compiled in Table 4. Representative EPR spectra are displayed in Figures 4 and 5. In general, the EPR spectra reveal the presence of a distorted tetragonal copper environment in the complexes with a $d_{x^2-y^2}$ ground state.[15,21] They are characterized by $g_\parallel > g_\perp$ and $|A_\parallel| > 120 \times 10$ cm^{-1}. An examination of the $g_\parallel$ and $|A_\parallel|$ values for complex **1** indicates that it possesses the highest value of $g_\parallel$ and lowest $|A_\parallel|$ value in the series. This is consistent with the binding of three nitrogen atoms and borders on Peisach and Blumberg[22] plots of $|A_\parallel|$ versus $g_\parallel$ for two nitrogens and two oxygens in the equatorial plane. This is in accordance with the X-ray results. No superhyperfine splittings from the ligand are observed (Figure 4).

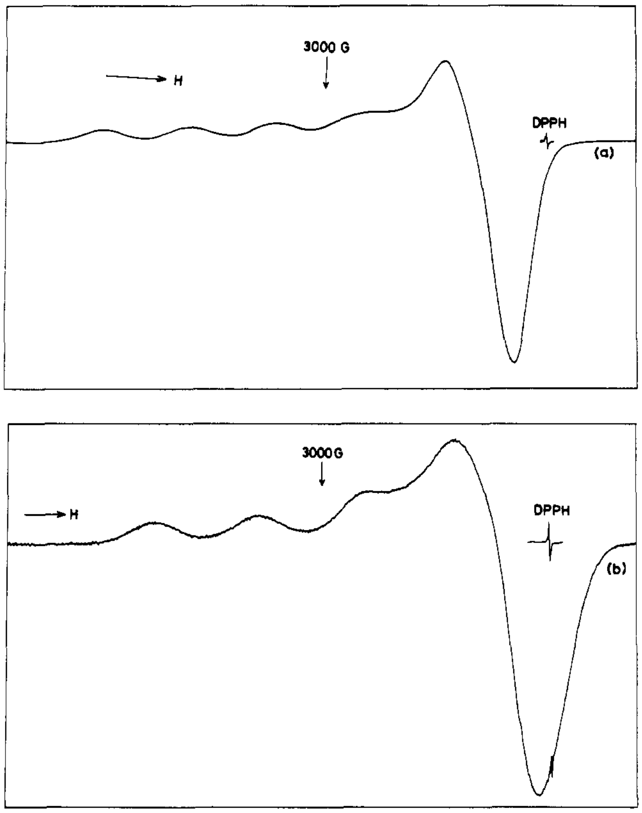

Figure 4. EPR spectra of polycrystalline powder samples of (a) **1** and (b) **3** at room temperature.

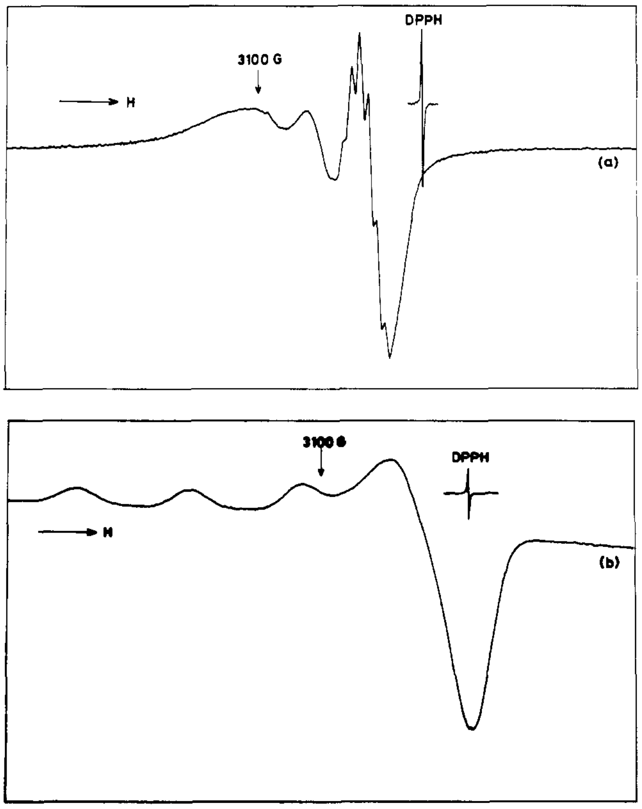

Figure 5. EPR spectra of compound **5** in dichloromethane at (a) room temperature and (b) liquid nitrogen temperature.

The EPR spectra of the ternary complexes **2**−**5** show less than four parallel lines and a broadening of the $g_\perp$ region. Such a broadening of the $g_\perp$ component is interpreted as indicative of lowered symmetry.[15] The increase in the $|A_\parallel|$ value indicates that the exogenous ligands enter the equatorial positions by displacing the water molecules.[23] The room-temperature solution EPR spectra of the complexes are isotropic with hyperfine splitting due to copper ($I = {}^3/_2$, approximately four lines). In addition, the bipyridine and phenanthroline adducts **4** and **5** display superhyperfine splitting due to coordinated nitrogens (Figure 5a). At liquid nitrogen temperature all mixed-ligand

---

(20) Balhausen, C. J. *Introduction to Ligand Field Theory*; McGraw-Hill: New York, 1963; pp 108, 185.

(21) Batra, G.; Mathur, P. *Inorg. Chem.* **1992**, *31*, 1575.

(22) Peisach, J.; Blumberg, W. E. *Arch. Biochem. Biophys.* **1974**, *165*, 691.

(23) (a) Reedijk, J. *Transition Met. Chem.* (*London*) **1981**, *6*, 195. (b) Okawa, H.; Busch, D. H. *Inorg. Chem.* **1979**, *18*, 1555.

complexes show axial pattern (see Figure 5b for example), with the $g_\parallel$ and $|A_\parallel|$ values characteristic of a square pyramidal geometry around copper.[24]

The g_{av} values for the complexes lie, with the exception of that for TPCTP·Cu(ClO$_4$)$_2$·2H$_2$O (**1**), in the range 2.109−2.143. Similar *g* factors were found for square pyramidal (*N*-salicylideneglycinato)- or (*N*-pyruvideneglycinato)copper(II) complexes having an additional ligand with N donors.[24,25] The g_{av} value of compound **1** is typical of elongated tetragonal complexes with tetrahedral distortion.[21] The *G* values for the present complexes are found to be greater than 4 (4.156−5.907) with the exception of that for TPCTP·Cu(ClO$_4$)$_2$·2H$_2$O. High *G* values indicate that the complexes are ionic.[26] The smaller value for **1** suggests the presence of coupling of Cu ions in coordination polyhedra.[15] The quotient $g_\parallel/|A_\parallel|$ has been considered as a convenient empirical index of tetrahedral distortion.[27] This quotient for complexes **1**−**5** ranges from 132 to 188 cm. It has been pointed out earlier that for square planar structures this occurs in the range from *ca.* 105 to 135 cm. This value increases markedly on the introduction of a tetrahedral distortion into the chromophore. Thus, the severely distorted complexes Cu[GaMe$_2$(Me$_2$Pz)$_2$]$_2$[28] and bis(*N-tert*-butylpyrrole-2-carbaldiminato)copper(II)[29] have values of 244 and 210 cm, respectively. The present complexes show values in the intermediate range, among them the aquo complex **1** having a higher quotient suggestive of a comparatively larger tetrahedral distortion.

A few points deserve attention: (i) While the effective charge on the equatorial plane remains constant, exchanging a less electron-rich O atom ligand for a more electron-rich nitrogen atom tends to lower $g_\parallel$ and increase $|A_\parallel|$ as we move in the series **1**−**5**. (ii) From aquo complex **1** to nitrogenous base adducts, both the increased covalency and relief in tetrahedral distortion are manifest in the increased $|A_\parallel|$ and lowered $g_\parallel$ values. (iii) Finally g_{av} values suggest a weaker axial interaction for these complexes, as is confirmed by the X-ray crystal structure determination of complexes **1** and **3**, where the axial positions are loosely bound by the cyclophosphazene ring nitrogen and a perchlorate anion.

In order to obtain a qualitative picture of the bonding nature in the complexes, we have calculated the LCAO−MO coefficients for the b_{1g} and b_{2g} orbitals, i.e., β_1^2 and β^2, which express the extents of in-plane and out-of-plane π bondings, respectively, and also the ligand coefficient α_{Cu}^2 for the b_{1g} MO. They are given in Table 5. The in-plane σ-covalency parameter α_{Cu}^2 was calculated using a simplified expression:[30,31]

$$\alpha_{Cu}^2 = \frac{-A_\parallel}{P} + (g_\parallel - g_e) + \frac{3}{7}(g_\perp - g_e) + 0.04$$

The α_{Cu}^2 values depend on the nature of copper−ligand bond, decreasing with increasing covalency (particularly in-plane σ bonding) to a minimum theoretical value of 0.50.[30] The observed values (0.73−0.80) account for the fraction of the unpaired electron density located on the copper. The unpaired electron is more localized toward ligands in the complexes which possess extra nitrogenous base ligands (**2**−**5**).

Table 5. Computed LCAO−MO Coefficients, Covalency Parameters, and Orbital Reduction Parameters

compd	medium	α^2	α_1^2	β_1^2	β^2	Fermi *K*
1	solid (rt)	0.79	0.29	0.89	0.76	0.33
	solid (lnt)	0.80	0.28	0.87	0.70	0.32
	CH$_2$Cl$_2$	0.79	0.30	0.76	0.67	0.30
	CH$_3$CN	0.77	0.32	0.99	0.76	0.32
2	solid (rt)	0.75	0.34	0.85	0.86	0.31
	solid (lnt)	0.74	0.35	0.82	0.94	0.31
	CH$_2$Cl$_2$	0.76	0.32	0.81	0.77	0.30
	CH$_3$CN	0.73	0.36	0.86	0.83	0.30
3	solid (rt)	0.76	0.33	0.80	0.63	0.30
	solid (lnt)	0.77	0.32	0.79	0.53	0.29
	CH$_2$Cl$_2$	0.73	0.36	0.85	0.78	0.31
	CH$_3$CN	0.76	0.33	0.74	0.78	0.28
4	solid (rt)	0.78	0.30	0.81	0.75	0.34
	solid (lnt)	0.76	0.33	0.77	0.64	0.33
	CH$_2$Cl$_2$	0.77	0.31	0.79	0.69	0.34
	CH$_3$CN	0.76	0.32	0.79	0.53	0.33
5	solid (rt)	0.77	0.32	0.83	0.70	0.33
	solid (lnt)	0.77	0.31	0.79	0.65	0.32
	CH$_2$Cl$_2$	0.76	0.32	0.79	0.54	0.32
	CH$_3$CN	0.76	0.32	0.79	0.63	0.32

Table 6. Electrochemical Data

		Cu^{II}−Cu^{I}		
compd	solvent	$E_{1/2}$, V	ΔE_p, mV	$E_{Cu^I-Cu^0}$
1	CH$_2$Cl$_2$	0.575	130	−1.24
	CH$_3$CN	+0.660	120	−0.45
2	CH$_2$Cl$_2$	+0.350[a]	*b*	−0.82
	CH$_3$CN	+0.450[a]	*b*	−0.58
3	CH$_2$Cl$_2$	−0.050[a]	*b*	−0.50
	CH$_3$CN	+0.210[a]	*b*	−0.65
4	CH$_2$Cl$_2$	+0.225	130	−0.75
	CH$_3$CN	+0.140[a]	*b*	−0.55
5	CH$_2$Cl$_2$	+0.215	90	−0.68
	CH$_3$CN	+0.225[a]	*b*	−0.63
		−0.050[a]	*b*	−1.02

[a] From differential pulse voltammograms. [b] Irreversible process.

The in-plane and out-of-plane metal π-bonding coefficients β_1^2 and β^2, respectively, are obtained from the following approximate equation:[31]

$$g_\parallel \simeq g_e + \frac{2\alpha^2\beta_1^2\lambda_0}{E_{xy}}; \qquad g_\perp \simeq g_e + \frac{8\alpha^2\beta^2\lambda_0}{E_{xzyz}}$$

The uncertainty involved in the assignment of the E_{xzyz} transition precludes a reliable estimate of the out-of-plane π-bonding parameter β^2. However, it is argued that the 20% error in E_{xzyz} results in only a ~5% error in β^2 values.[30] The complexes studied show β_1^2 = 0.74−0.99, indicating a covalent in-plane π bonding. Again, weaker in-plane π bonding is proposed for the aquo complex (**1**) on the basis of larger β_1^2 values. This is also supported by the comparatively larger orbital reduction factors for complex **1**.

Electrochemistry. The electrochemical behavior of complexes **1**−**5** has been examined by cyclic voltammetric and differential pulse voltammetric studies in dichloromethane and acetonitrile solutions. The data are given in Table VI.

The aquo complex **1** shows a quasireversible Cu(II)−Cu(I) redox couple at *ca.* +0.6 V (Figure 6a) in both dichloromethane

---

(24) (a) Plesch, G.; Friebel, C.; Švajlenová, O.; Krätsmár-Šmogrovič, J. *Inorg. Chim. Acta* **1987**, *129*, 81. (b) Plesch, G.; Friebel, C.; Švajlenová, O.; Krätsmár-Šmogrovič, J. *Polyhedron* **1991**, *10*, 893.

(25) Plesch, G.; Friebel, C.; Švajlenová, O.; Krätsmár-Šmogrovič, J.; Mlynarčíck, D. *Inorg. Chim. Acta* **1988**, *151*, 139.

(26) Friebel, C. *Z. Naturforsch.* **1974**, *29B*, 295.

(27) Sakaguchi, U.; Addison, A. W. *J. Chem. Soc., Dalton Trans.* **1979**, 600.

(28) Herring, D. G.; Patmore, D. J.; Storr, A. *J. Chem. Soc., Dalton Trans.* **1975**, 711.

(29) Yokoi, H.; Addison, A. W. *Inorg. Chem.* **1977**, *16*, 1341.

(30) (a) Kivelson, D.; Nieman, R. *J. Chem. Phys.* **1961**, *35*, 149. (b) Maki, A. K.; McGarvey, B. R. *J. Chem. Phys.* **1958**, *29*, 31.

(31) Billing, D. E.; Hathaway, B. J.; Nicholls, P. *J. Chem. Soc. A* **1969**, 316.

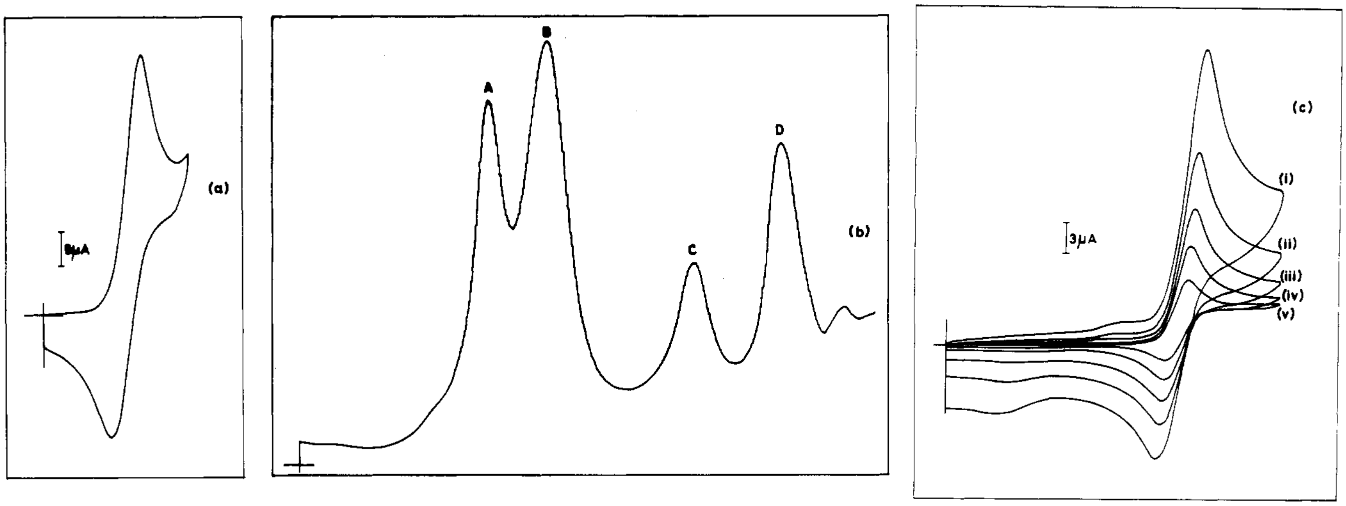

Figure 6. (a) Cyclic voltammogram of compound **1** recorded in dichloromethane solution (initial potential +1.0 V, final potential +0.4 V, scan rate 50 mV/s). (b) Differential pulse voltammogram of **5** recorded in acetronitrile solution (initial potential +1.0 V, final potential −1.4 V, scan rate 10 mV/s). (c) Cyclic voltammograms of compound **4** in dichloromethane solution recorded at various scan rates (initial potential +1.2 V, final potential −0.2 V): (i) 500 mV/s; (ii) 200 mV/s; (iii) 100 mV/s; (iv) 50 mV/s; (v) 20 mV/s.

and acetonitrile solutions, corroborating the increased tetrahedral distortion suggested by the EPR parameters as well as X-ray diffraction studies. Similarly, the quasireversibility of the bipyridine and phenanthroline adducts in dichloromethane solutions indicates that there is no appreciable structural change involved prior to reduction of copper(II) complexes. However, in acetonitrile solution an irreversible Cu(II)−Cu(I) redox change is observed for all the nitrogen base adducts. After the one-electron reduction, these complexes in acetonitrile solution probably undergo rapid decomposition. Invariably all the complexes show an irreversible one-electron reduction at *ca.* −0.6 to −1.2 V attributable to the Cu(I)−Cu(0) change. On reversal of the scan, all complexes exhibit a strong stripping peak characteristic of the reoxidation of the *naked* metal. The redox behavior of complexes **1**, **3**, and **4** in dichloromethane solution may be so schematized as

$$\begin{tikzcd}
{[TPCTP\cdot Cu^{II}\cdot L_n]^{2+}} \arrow[r, shift left, "e"] & {[TPCTP\cdot Cu^{I}\cdot L_n]^{+}} \arrow[l, shift left, "e"] \arrow[r, "e"] & {[TPCTP\cdot Cu^{0}\cdot L_n]^{0}} \arrow[d, "\text{fast}"] & \\
 & & L_n + TPCTP + Cu^{0} \arrow[r] & Cu^{+}
\end{tikzcd}$$

In acetonitrile solution a different mechanism may be operating with the likely expulsion of the extra ligands from the coordination sphere in an attempt to achieve a more comfortable tetrahedral geometrical arrangement to stabilize the Cu(I) species generated. The coordinating ability of acetonitrile may be the driving force for this kind of mechanism. The differential pulse voltammogram of complex **5** in acetonitrile solution is presented in Figure 6b, which is compatible with the following mechanism:

$$\begin{tikzcd}
{[TPCTP\cdot Cu^{II}\cdot L_n]^{2+}} \arrow[r, "\text{peak A}", "+e"'] & {[TPCTP\cdot Cu^{I}\cdot L_n]^{+}} \arrow[r, shift left, "\text{peak B}"] \arrow[d, "+e\ \text{peak C}"] & {[TPCTP\cdot Cu^{I}\cdot (sol)_2]^{+}} \arrow[l, shift left] \arrow[d, "+e\ \text{peak D}"] \\
 & {[TPCTP\cdot Cu^{0}\cdot L_n]^{0}} & {[TPCTP\cdot Cu^{0}\cdot (sol)_2]^{0}}
\end{tikzcd}$$

It is probable that in dichloromethane the preferred geometry for the copper(I) intermediates may be a five-coordinate distorted trigonal bipyramid. However, this conclusion awaits the structural characterization of at least one copper(I) complex. Our attempts to isolate stable copper(I) complexes using this ligand have not been successful so far.

We can draw the following conclusions: (i) The imidazole (**3**) and pyridine (**2**) adducts are not redox flexible owing to the observation of irreversible Cu(II)−Cu(I) reduction both in dichloromethane and in acetonitrile solutions. (ii) The high positive redox potential observed for the Cu(II)−Cu(I) redox change for the aquo complex (**1**) compared with the bipyridine (**4**) and phenanthroline (**5**) adducts may arise from the increased tetrahedral distortion in the former, which would stabilize the Cu(I) congener,[32] and from the electronic effects prevalent because of the replacement of two less electron aquo ligands by electron-rich bipyridine or phenanthroline ligands, which hampers the addition of electrons to the metal. (iii) The conventional analysis of the Cu(II)−Cu(I) peak systems of complexes **1**, **4**, and **5** exhibited in dichloromethane solutions with scan rates varying from 0.02 to 1.0 V/s shows that the peak-to-peak separation increases progressively from *ca.* 0.08 to 0.28 V. This maximum departure from the constant value of 0.059 V expected for an electrochemically reversible one-electron transfer denotes that a considerable geometrical reorganization accompanies the Cu(II)−Cu(I) redox change.[32]

Conclusions

The spectral and structural properties of the mixed-ligand complexes TPCTP·Cu(ClO$_4$)$_2$·*n*L (**1**−**5**) resulting from a pyrazolylcyclotriphosphazene ligand, $N_3P_3Ph_2(3,5\text{-}Me_2Pz)_4$, show a significant dependence on the nature of the additional ligand(s). When L = H_2O ($n = 2$), the copper assumes an elongated tetragonal geometry, and the imidazole analogue shows a distorted square pyramidal geometry for copper. EPR results indicate that there exists an interesting compensation between the tetrahedral distortion and electronic effects. Thus, in TPCTP·Cu(ClO$_4$)$_2$·2H$_2$O (**1**) the tetrahedral distortion decreases $|A_{\parallel}|$ and increases the $g_{\parallel}$ value while in TPCTP·Cu(ClO$_4$)$_2$·Bipy (**4**) the presence of an electron-rich bipyridine increases mark-

---

[32] Zanello, P. In *Stereochemistry of Organometallic and Inorganic Compounds*; Bernal, I., Ed.; Elsevier: Amsterdam, 1990; Vol. 4, p 181.

edly the $|A_{\parallel}|$ value and lowers the $g_{\parallel}$ value. Similar effects are observable in the electrochemical properties of the complexes also. Although the N_3 coordination mode is retained in TPCTP, it forms only the mononuclear complexes, in contrast to the hexasubstituted analogue HPCTP, which yields both mono- and dinuclear complexes. All these results suggest that the electronic changes in the cyclophosphazene moiety would also influence the outcome of the properties of the resulting complexes. Work in this direction is in progress to evaluate the effect of nature of substituents in cyclophosphazene as well in pyrazolyl moieties by designing a cyclotriphosphazene ligand containing only two coordinating pyrazolyl groups.

Acknowledgment. We thank the Department of Science and Technology, New Delhi, India, for generous financial support. K.R.J.T. thanks the Indian Institute of Technology, Kanpur, India, for a research fellowship. Technical assistance rendered by Mr. Ahmed and Mr. Kanaujia is gratefully acknowledged.

Supplementary Material Available: Listings of atomic coordinates, anisotropic thermal parameters, bond distances and angles, least-squares planes, and torsion angles for **1** and **3** and simulated EPR spectra of polycrystalline powder samples of **1** (Figure 4c) and of **5** (Figure 5c) (23 pages). Ordering information is given on any current masthead page.